Supplementary information for: *Effect of sodium silicate on drinking water biofilm development*

This document contains 6 figures, 2 tables, and 12 pages.

Pilot-scale model distribution system

General water quality

Figure 1 summarizes free chlorine, pH, phosphate residual, silica residual, and TOC, while Figure 2 summarizes aluminum, true colour, iron, manganese, total nitrogen, turbidity, and UV_{254}. Both figures represent samples collected from the influent and effluent of each AR.

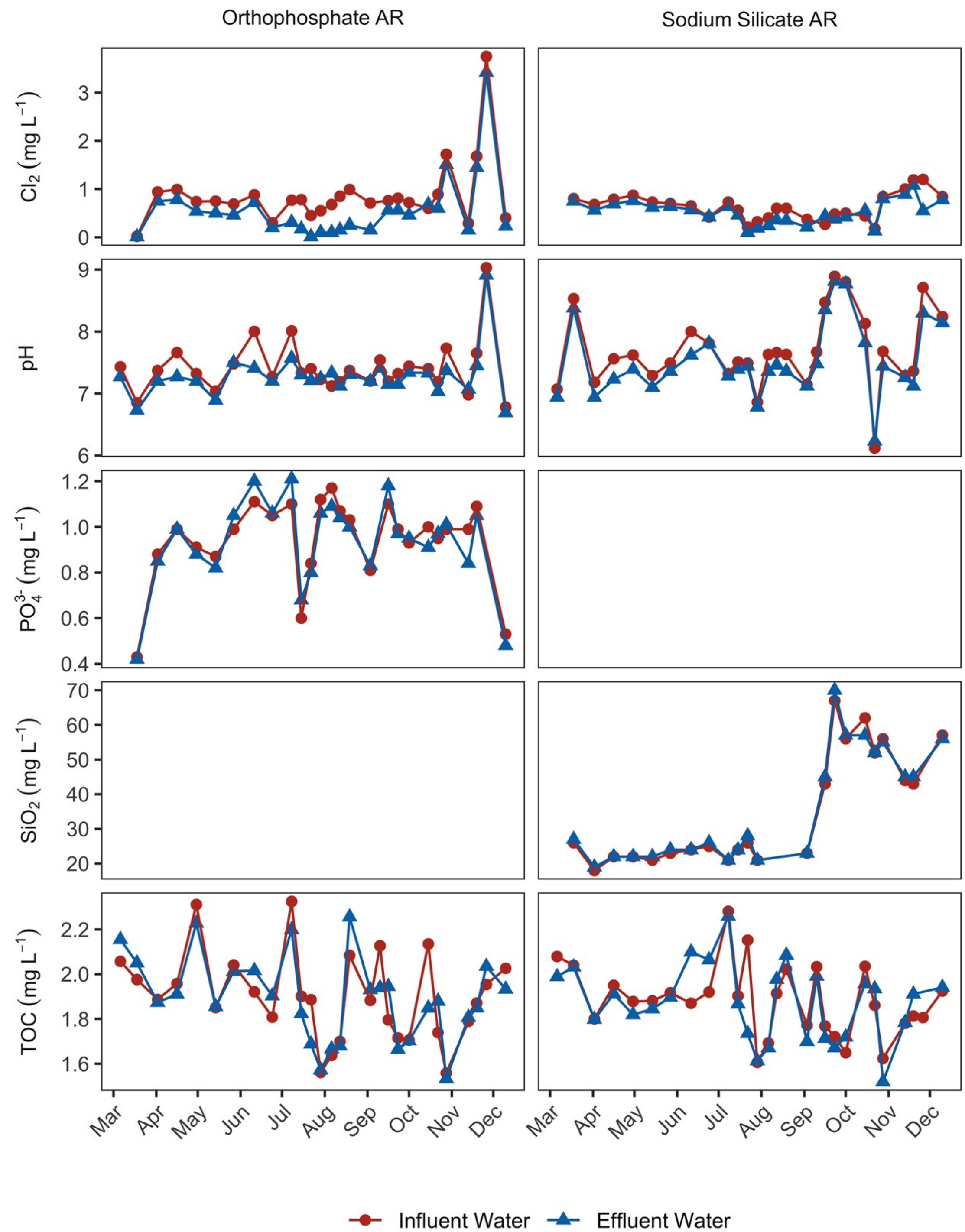

Figure 1: Free chlorine, pH, phosphate residual, silica residual, and TOC measured in the influent (reservoir) and effluent water of each AR. The drop in pH in the influent/effluent of the silicate-treated AR represents an overcorrection (pH was adjusted in an attempt to maintain a stable target pH of 7.4 after doubling the sodium silicate dose).

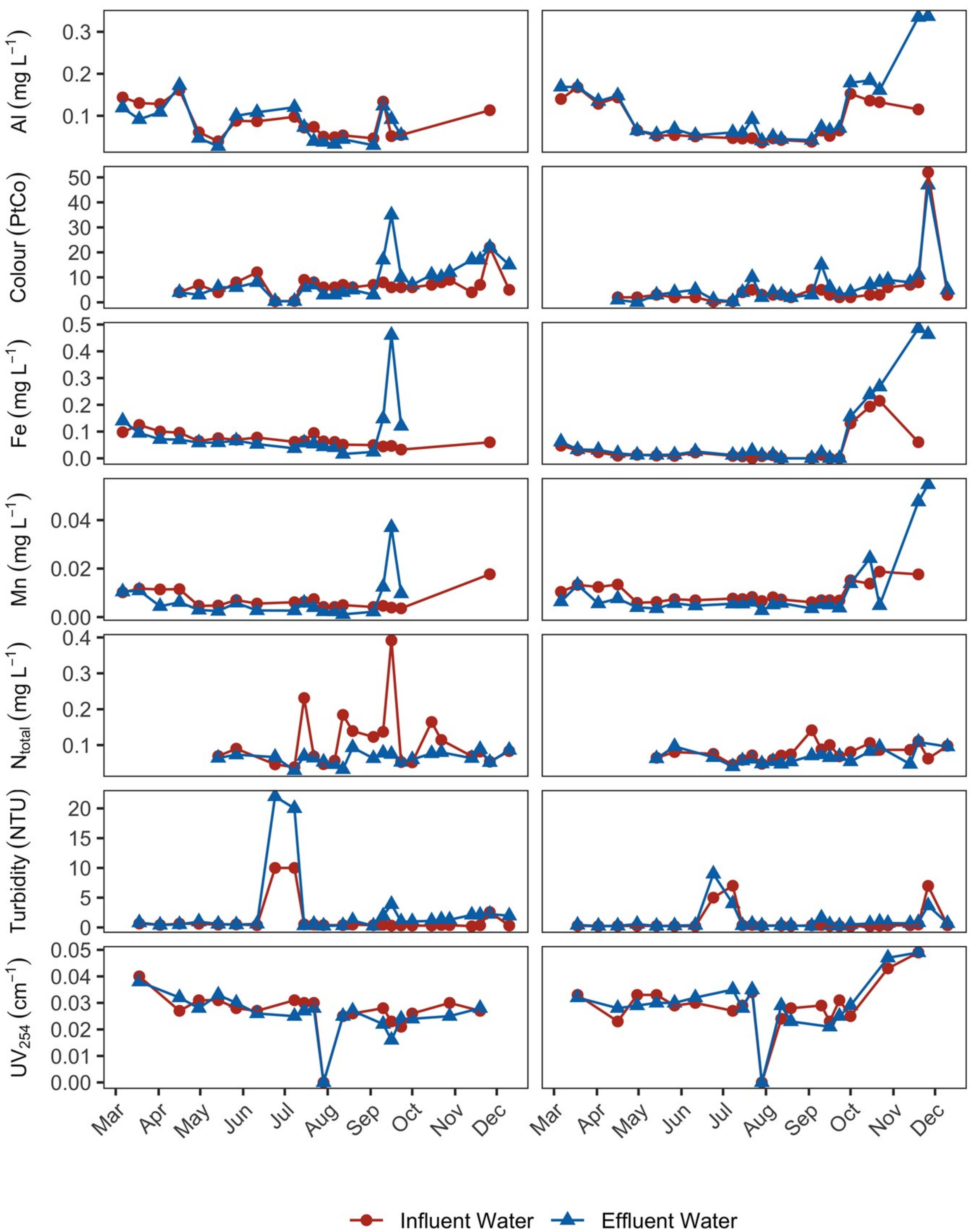

16

17 *Figure 2: Aluminum, true colour, iron, manganese, total nitrogen, turbidity, and UV_{254}*
18 *measured in the influent (reservoir) and effluent water of each AR.*

Free chlorine

During the full extent of the study median influent free chlorine concentrations in the orthophosphate AR were 0.76 mg L^{-1} (range: 0.02 - 3.75 mg L^{-1}, n = 26) and in the sodium silicate AR were 0.63 L^{-1} (range: 0.18 - 1.20 mg L^{-1}, n = 26). The orthophosphate-treated system experienced a higher chlorine reduction across the AR, especially during the July - September quarter (Q2). The corresponding mean free chlorine reductions during Q2 were 69.6% in the orthophosphate AR, and 24.6% in the sodium silicate AR.

pH

The pH of the influent water samples gathered during the study ranged from a median of 7.35 (range: 9.03 - 6.78, n = 28) for the orthophosphate AR, to 7.63 (range: 8.89 - 6.12, n = 28) for the sodium silicate AR. The differences in pH between both systems were not significantly different at the 95% confidence level. In the sodium silicate-treated AR there was a noticeable increase in pH at the beginning of Q3 (September - December) when the sodium silicate dose increased in the pipe loop systems (September 05, 2019). This effect is explained by the alkaline nature of this type of corrosion inhibitor.

Phosphate and silica residual

The median phosphate residual concentrations in the influent water were stable through each quarter in contrast with the sodium silicate-treated system, mainly due to the adjustment to a higher silica residual target from 24 to 48 mg L^{-1} in September 05, 2019. The median phosphate residual concentrations were 0.99 mg L^{-1} (range: 1.17 - 0.43 mg L^{-1}, n = 25), and the silica residual concentrations were 25.5 mg L^{-1} (range: 67.00 - 18.00 mg L^{-1}, n = 22).

Temperature

Influent water temperatures recorded for each reactor system demonstrated seasonal variation, as expected. Median water temperatures were higher during Q2 (July - September) within each system, reaching median temperatures of 20.5 and 20.0 °C for the orthophosphate and sodium silicate-treated systems, respectively. The median influent water temperatures during this study were 18.0 °C (range: 23.00 - 12.00 °C, n = 29) and 17.5 °C (range: 22.50 - 12.00 °C, n = 29), respectively.

Batch Reactors

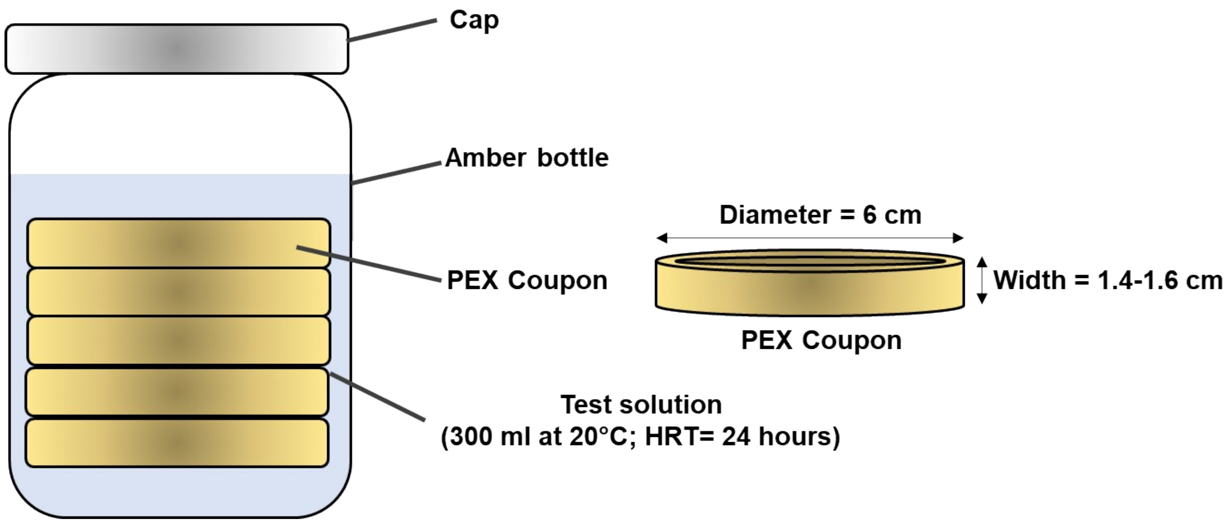

Figure 3: Simplified schematic of the batch reactors.

Microbial community structure

Taxonomic analysis

The mayor ASVs identified at the phylum level were *Proteobacteria*, *Bacteroidetes*, *Firmicutes*, *Actinobacteria*, *Cyanobacteria*, and *Euryarchaeota* (Figure 2). At this phylum level, the presence of *Proteobacteria* dominated the community structure in both orthophosphate and sodium silicate-treated systems (> 74% for every month expect for November). The presence of *Proteobacteria* was dominant from June to October until a shift in the bacterial community structure occurred in November 2019, allowing the identification of *Bacteroidetes*, *Firmicutes*, *Actinobacteria*, *Cyanobacteria*, and *Euryarchaeota*. A similar presence of organisms at the phylum level have been reported in drinking water biofilm studies using a variety of substrate materials, including ductile cast-iron, stainless steel, tuberculated cast-iron, and PVC.[1–5] Generally, *Proteobacteria*, *Firmicutes*, *Actinobacteria*, and *Bacteroidetes* have been associated with the culturable portion of phosphate treated water on ductile cast-iron and stainless steel coupons;[2] the same phyla were detected on both orthophosphate and sodium silicates treated cast-iron systems, however their relative abundance (with the expection of *Proteobacteria*) was higher in the orthophosphate-treated system.

The most noticeable difference at the phylum level between both orthophosphate and sodium silicate-treated systems is the presence of *Cyanobacteria* from the sodium silicate system in November, and the detection of *Euryarchaeota* from the orthophosphate system, aslo in November. Douterelo *et al.*[1], reported that *Cyanobacteria* were positively correlated with TOC levels and was present in plastic pipes during the winter months (low water temperatures), which may suggest that with an absence of phosphorus in the sodium silicate-treated system *Cyanobacteria* was able to assimilate available carbon more effectively.

At the genus level the abundance of *Phreatobacter* was higher in the orthophosphate system (identified from June through December, except for November), than in the sodium silicate system (Figure 5). According to Perrin *et al.*[5], the presence of *Phreatobacter* in drinking water distribution systems is related to warm water temperatures (>15 °C).

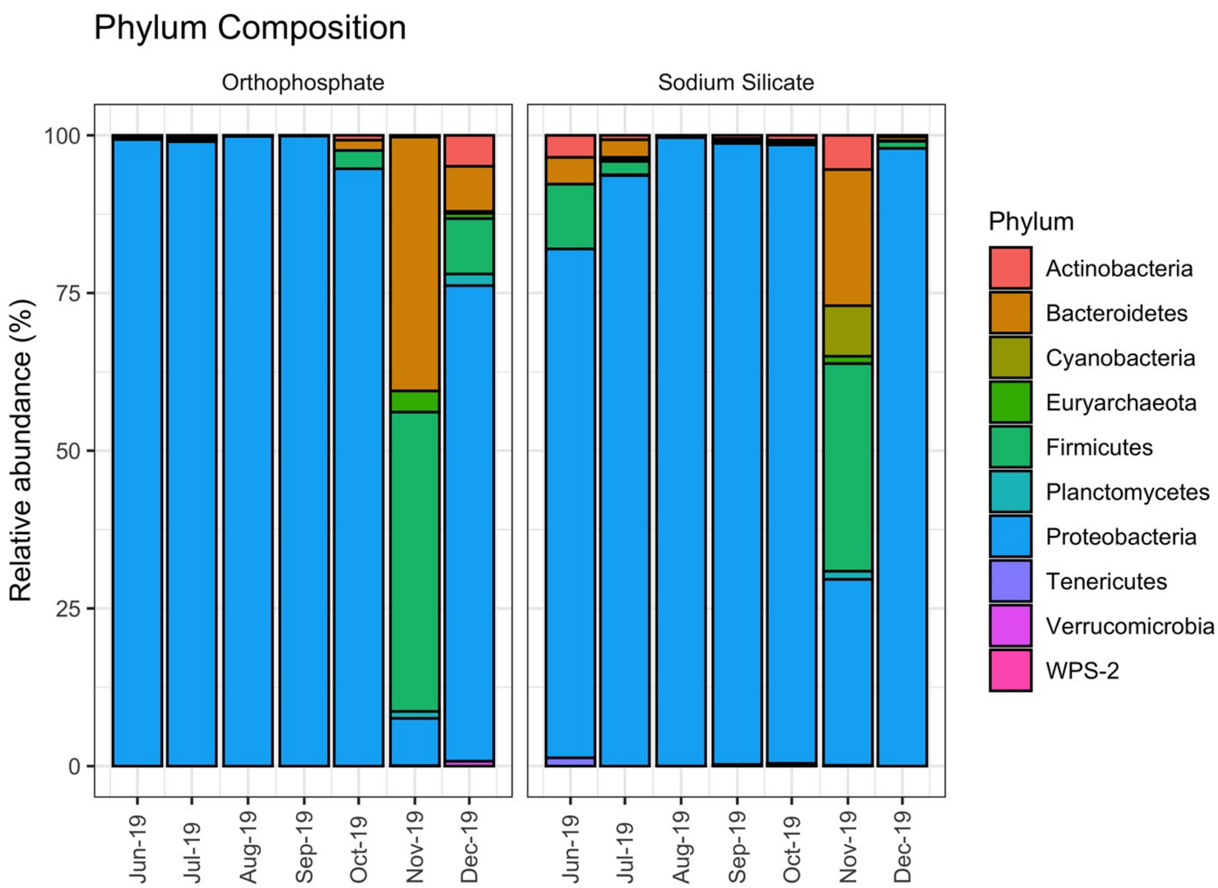

Figure 4: Relative abundance at the phylum level of bacterial community structure.

Table 1: Relative abundance (%) summary of genera associated with MOB and pathogenic bacteria species identified from the sodium silicate and orthophosphate-treated AR coupons during the months of June - December 2019.

Month	Inhibitor	Escherichia-Shigella	Halomonas	Hyphomicrobium	Legionella	Mycobacterium	Sphingomonas
Jun	P	-	-	-	-	-	1.6
Jul	P	-	0.1	0.2	-	0.2	3.2
Aug	P	-	0.0	0.0	-	0.0	10.2
Sep	P	0.0	-	0.0	0.0	0.0	15.8
Oct	P	0.2	0.6	0.2	-	0.4	9.6
Nov	P	-	7.6	-	-	-	-
Dec	P	0.1	0.5	0.9	0.1	3.3	7.9
Jun	Si	0.2	-	4.8	-	0.3	5.7
Jul	Si	-	-	2.8	-	0.6	14.4
Aug	Si	-	-	0.3	-	0.0	2.0
Sep	Si	-	0.0	0.2	0.0	0.0	0.9
Oct	Si	-	0.0	0.2	0.2	0.1	34.3
Nov	Si	0.6	1.9	-	0.2	1.7	7.8
Dec	Si	-	0.0	0.3	-	-	8.0

Table 2: Absolute abundances of genera associated with MOB and pathogenic bacteria species identified from the sodium silicate and orthophosphate-treated AR coupons during the months of June - December 2019.

Month	Inhibitor	Escherichia-Shigella	Halomonas	Hyphomicrobium	Legionella	Mycobacterium	Sphingomonas
Jun	P	-	-	-	-	-	843
Jun	Si	22	-	462	-	33	552
Jul	P	-	62	67	-	80	1449
Jul	Si	-	-	577	-	122	3001
Aug	P	-	21	13	-	3	17093
Aug	Si	-	-	414	-	26	2447
Sep	P	2	-	13	7	14	32735
Sep	Si	-	7	58	15	3	305
Oct	P	23	58	20	-	42	925
Oct	Si	-	4	116	93	74	20487
Nov	P	-	775	-	-	-	-
Nov	Si	14	43	-	5	39	175
Dec	P	6	39	65	9	239	574
Dec	Si	-	6	66	-	-	1591

Alpha and beta diversity analysis

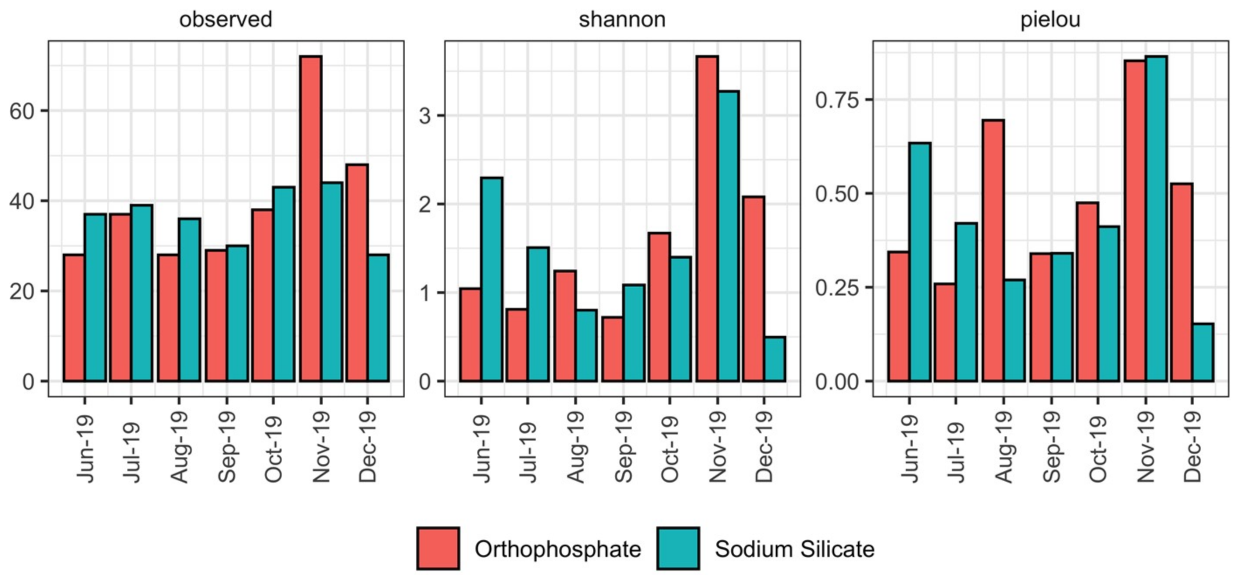

Figure 5: Richness, Shannon diversity index, and Pielou evennes index in biofilm samples collected from June to December 2019.

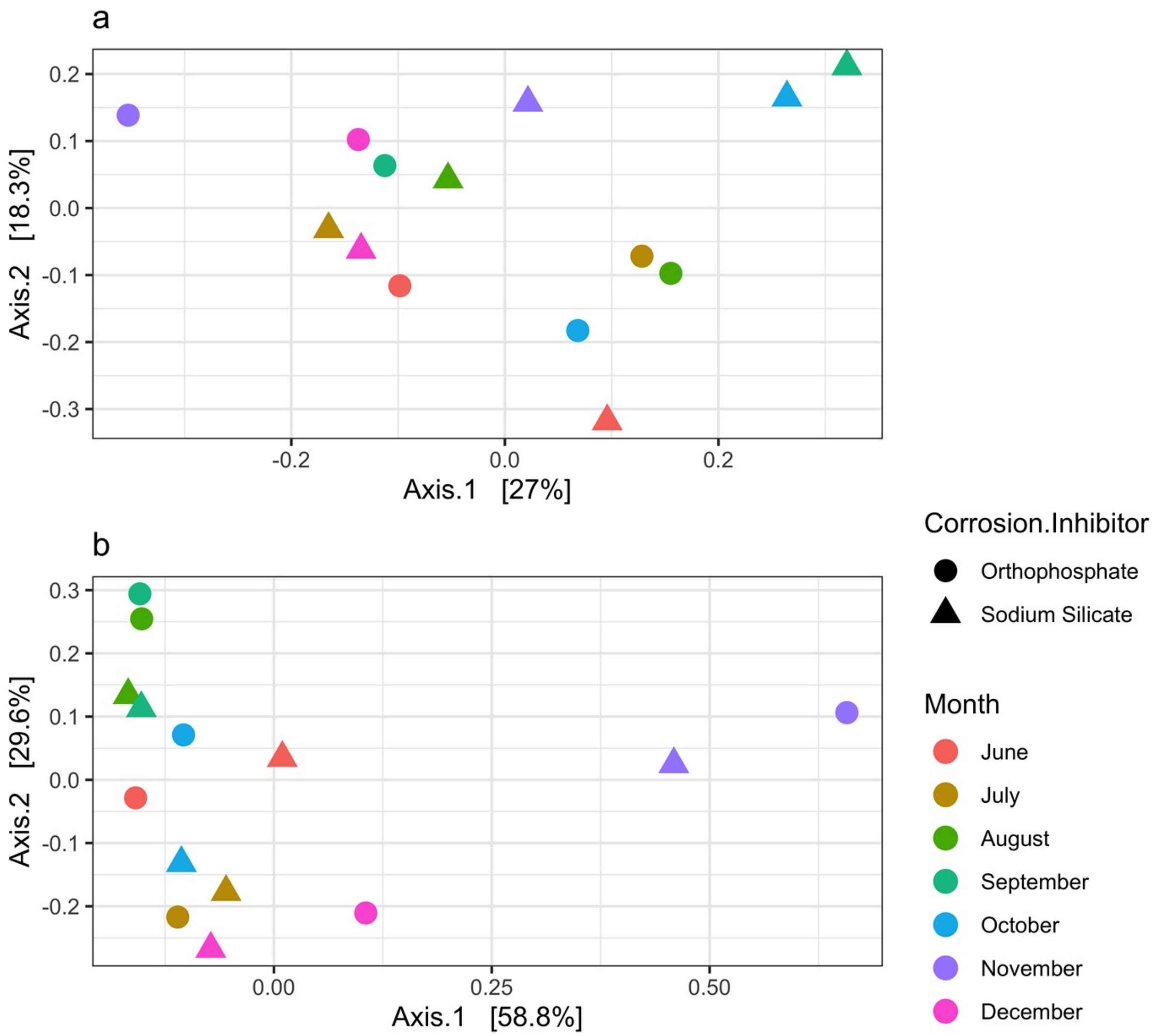

Figure 6: (a) Principle coordinate analysis for unweighted and (b) weighted UniFrac distances.

References

1 I. Douterelo, S. Husband, V. Loza and J. Boxall, Dynamics of biofilm regrowth in drinking water distribution systems, *Applied and Environmental Microbiology*, 2016, **82**, 4155–4168.

2 H. J. Jang, Y. J. Choi, H. M. Ro and J. O. Ka, Effects of phosphate addition on biofilm bacterial communities and water quality in annular reactors equipped with stainless steel and ductile cast iron pipes, *Journal of Microbiology*, 2012, **50**, 17–28.

3 A. C. Martiny, H.-J. Albrechtsen, E. Arvin and S. Molin, Identification of Bacteria in Biofilm and Bulk Water Samples from a Nonchlorinated Model Drinking Water Distribution System-Nitrospira.pdf, *Applied and Environmental Microbiology*, 2005, **71**, 8611–8617.

4 S. J. Payne, G. S. Piorkowski, L. T. Hansen and G. A. Gagnon, Impact of zinc orthophosphate on simulated drinking water biofilms influenced by lead and copper, *Journal of Environmental Engineering*, 2016, **142**, 1–9.

5 Y. Perrin, D. Bouchon, V. Delafont, L. Moulin and Y. Héchard, Microbiome of drinking water: A full-scale spatio-temporal study to monitor water quality in the Paris distribution system, *Water Research*, 2019, **149**, 375–385.